Applied Thermal Engineering 111 (2017) 1401–1408

Contents lists available at ScienceDirect

Applied Thermal Engineering

journal homepage: www.elsevier.com/locate/apthermeng

Research Paper

Cross-plane heat conduction in nanoporous silicon thin films by phonon Boltzmann transport equation and Monte Carlo simulations

Yu-Chao Hua (华钰超), Bing-Yang Cao (曹炳阳)*

Key Laboratory for Thermal Science and Power Engineering of Ministry of Education, Department of Engineering Mechanics, Tsinghua University, Beijing 100084, China

HIGHLIGHTS

- A model for cross-plane thermal conductivity of nanoporous films is proposed by BTE.
- Our model captures the effects for thickness, pore radius and porosity simultaneously.
- A MC method is developed to simulate phonon transport in nanoporous Si films.
- Good agreements between the present model and MC simulations have been achieved.

GRAPHICAL ABSTRACT

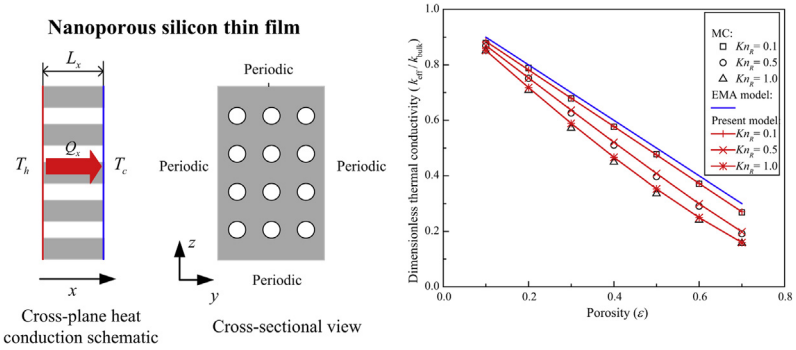

ARTICLE INFO

Article history:
Received 10 March 2016
Revised 22 May 2016
Accepted 25 May 2016
Available online 1 June 2016

Keywords:
Thermoelectric
Nanoporous silicon thin film
Effective thermal conductivity
Phonon Boltzmann transport equation
Monte Carlo
Phononic crystals

ABSTRACT

The study on the heat conduction in nanoporous silicon structures has drawn much attention due to their significance for developing highly-efficient thermoelectric materials. In the nanostructures whose characteristic lengths are comparable to the phonon mean free path (MFP), ballistic transport and boundary scattering will lead to the size-dependence of effective thermal conductivity. In the present work, the cross-plane thermal transport along the pore axial direction in nanoporous silicon thin films (i.e. silicon thin films crossed by nanoscale cylindrical channels) is investigated by using the phonon Boltzmann transport equation (BTE) and the Monte Carlo (MC) simulations. It is found that the effective thermal conductivity varies not only with the porosity but also with the film thickness and pore radius. The smaller the film thickness or the pore radius, the smaller is the effective thermal conductivity for a given porosity. An analytical model for the cross-plane effective thermal conductivity of nanoporous silicon thin films is obtained on the basis of the phonon BTE. The model can capture the size effects due to the film thickness and the pore radius simultaneously, and be reduced to the Fourier's law based model for macroporous materials. Good agreements have been achieved between the present model and the MC simulations. Our model can be useful for predicting and controlling phonon transport for thermoelectric devices.

1. Introduction

The developments of green technologies, e.g., waste heat recovery, push researchers to study highly-efficient thermoelectric devices [1,2]. The efficiency of thermoelectric materials is dependent on the dimensionless thermoelectric figure of merit [3], $ZT = S^2\sigma T/k$, where S is the Seebeck coefficient, σ is the electrical conductivity, k is the thermal conductivity, and T is the absolute temperature. The key to improving the efficiency of thermoelectric devices is to reduce the thermal conductivity without adversely influencing the electrical conduction ability. Many innovative ideas

* Corresponding author.
E-mail address: caoby@mail.tsinghua.edu.cn (B.-Y. Cao).

http://dx.doi.org/10.1016/j.applthermaleng.2016.05.157
1359-4311/

have been proposed to increase ZT based on the engineering of electron and phonon transport [4,5]. Nanoporous silicon structures [6] have demonstrated great potential in new generation thermoelectric materials [7]. Researchers found that by etching nanoscale holes in silicon thin films (i.e. silicon thin films crossed by nanoscale cylindrical channels) the effective thermal conductivity can be greatly reduced, while only a minor effect occurs on the electrical properties of silicon. In this way, the figure of merit can be significantly improved. Therefore, the study on the thermal transport in nanoporous silicon thin films becomes necessarily essential for the further development of highly-efficient thermoelectric devices.

Phonons predominate the heat conduction in silicon [8]. In nanostructures whose characteristic lengths are comparable to the phonon mean free path (MFP), ballistic transport and boundary scattering will make the effective thermal conductivity dependent on geometry and size [9,10], indicating a violation of classical Fourier's law of heat conduction, so the Fourier's law based model for the effective thermal conductivity of macro-porous materials can be invalid [11]. Generally, the phonon Boltzmann transport equation (BTE) is employed to characterize the nanoscale thermal transport [10],

$$\vec{v}_g \cdot \nabla f = \frac{f_0 - f}{\tau}, \tag{1}$$

where $\vec{v}_g$ is the group velocity, f is the phonon distribution function, f_0 is the equilibrium distribution function, and τ is the relaxation time.

Many researches have devoted to investigating the effective thermal conductivity of nanoporous silicon thin films both theoretically and experimentally. It has been found that the effective thermal conductivity of nanoporous thin films can significantly reduce as compared to that of macroporous materials, and increase with the increasing characteristic lengths, e.g. film thickness and pore radius. Yang et al. [11] numerically studied the thermal transport along the pore axial direction in the nanoporous structures through solving the phonon BTE, and found the pore radius dependence of effective thermal conductivity. Hsieh et al. [12] employed a frequency-dependent phonon BTE solver to investigate the thermal transport perpendicular to the pore axial direction, and discussed the influence of pore geometries on the transverse thermal conductivity of nanoporous silicon. Tang et al. [13] numerically studied the influence of film thickness and pore structure on the transverse thermal conductivity of nanoporous films based on the phonon BTE. Besides, molecular dynamics (MD) simulation is an important numerical technique to investigate the nanoscale thermal transport. Lee et al. [14] used the MD technique to study the thermal properties of nanoporous silicon. Based on the MD simulations, Fang and Pilon [15] proposed that the effective thermal conductivity of nanoporous silicon can be tuned by surface passivation. Except for the numerical solution of phonon BTE and the MD simulations, the Monte Carlo (MC) method is another widely-adopted numerical technique to study the phonon transport in nanoporous silicon structures. Randrianalisoa and Baillis [16] applied the MC technique to predict the effects of porosity, pore sizes, pore arrangement, temperature, and film thickness on the cross-plane thermal conductivity of nanoporous silicon films. Liu and Huang [17] and Wolf et al. [18] investigated the transverse thermal conductivity of nanoporous silicon using the MC simulations. As for experiments [18–22], Yu et al. [19] and Alaie et al. [20] measured the in-plane effective thermal conductivity of nanoporous silicon films in the transverse direction (that is, the direction perpendicular to the pore axis), proving the significant reduction of thermal conductivity. Hopkins et al. [21] and Weisse et al. [22] measured the cross-plane thermal conductivity along the pore axial direction of nanoporous silicon films using the time domain thermoreflectance method, demonstrating the influence of diameter and porosity on effective thermal conductivity. Lee et al. [23] measured the cross-plane thermal conductivity of nanoporous silicon thin films along the pore axial direction, and mainly analyzed the film thickness dependence of effective thermal conductivity.

Numerical and experimental results uncovered the variation rules of the effective thermal conductivity of nanoporous silicon structures, and promoted the development of relevant theoretical models [24–27]. Prasher [24] proposed an approximate ballistic-diffusive effective medium model for the transverse thermal conductivity of nanoporous films as an alternative of the phonon BTE. Liu and Huang [17] modified Prasher's model and discussed the effect of pore geometries on the transverse thermal conductivity. Prasher [25] then derived a theoretical model of thermal conductivity along the pore axial direction for nanoporous films with infinite thickness based on the phonon BTE. Alvarez et al. [26] used phonon hydrodynamics to analyze the influence of porosity and pore size on reduction of effective thermal conductivity in porous silicon. Dettori et al. [27] obtained a phenomenological model for the transverse thermal conductivity of nanoporous silicon from the MD simulations. Besides, the changes of phonon properties resulted from the phononic crystal patterning have also been regarded as important factors for the reduction of effective thermal conductivity [20,21,28]. It should be noted that most of modeling works at present are based on the phenomenological methodologies [24,27], and cannot simultaneously take multiple geometrical constraints into account. A more in-depth understanding about the thermal transport in nanoporous silicon thin films and the corresponding predictive model are still desired.

In the present work, we study the cross-plane heat conduction along the pore axial direction in the nanoporous thin films by using the phonon BTE and the MC simulations. The analytical model for the cross-plane effective thermal conductivity of nanoporous thin films is derived from the phonon BTE and verified by comparison with the MC simulations.

2. Problem formulation

Fig. 1 illustrates the schematic for the cross-plane heat conduction in nanoporous silicon thin films. The film thickness is L_x, the pore radius is R_p, and the distance between two neighboring pore axials is L_p. The temperature difference is applied along the pore axial direction (x direction), and thus the thermal transport is periodic in the y- and z-directions. Therefore, the phonon transport inside the nanoporous thin films can be represented by that in the unit cell shown in Fig. 2(a) with the totally specular scattering boundary conditions in the y- and z-boundaries [11,24,25]. It should be note that the specular scattering boundary conditions in the y- and z-boundaries do not change the transport direction of phonon energy, resulting in the same influence on effective thermal conductivity as that caused by the periodic boundary conditions. In our studying cases, pores are squarely arrayed in nanofilms, and thus the maximum porosity in theory is equal to $\pi/4 \approx 0.79$. In reality the nanoporous thin films may hold various pore-array patterns, but this issue cannot significantly influence the cross-plane effective thermal conductivity for the given porosity and characteristic lengths [11]. For simplicity and clarity, following the method of Yang et al. [11], the outer surface of the square unit cell is converted into a circle, that is, to approximate a square unit cell cross section as a circular cross section with the same cross-sectional area (shown in Fig. 2(b)), $R_o = L_p/\sqrt{\pi}$, and the porosity is then calculated as $\varepsilon = R_p^2/R_o^2$. The x-directional isothermal boundaries are set as phonon blackbody boundaries, i.e. phonons arriving at these boundaries will be completely absorbed [29]. Besides, the pore boundary is thermally adiabatic,

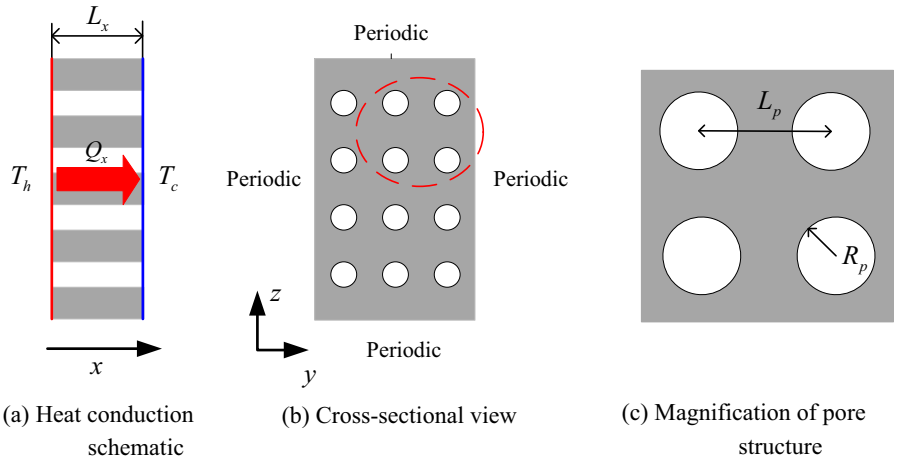

Fig. 1. Schematic for cross-plane heat conduction in nanoporous silicon thin films: the film thickness is denoted by L_x, the direction of heat flow, Q_x, is parallel with the pore axial, the pore radius is R_p, and the distance between two neighboring pore axials is L_p.

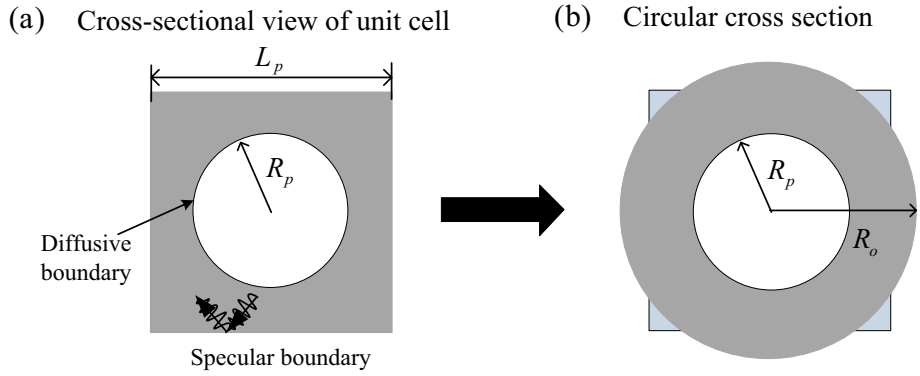

Fig. 2. Cross-sectional view of a unit cell (a): a square unit cell cross section is approximated as a circular cross section (b), and $R_o = \frac{L_p}{\sqrt{\pi}}$.

that is, all phonons that strike it will be reflected back to the domain. A specular parameter, P, has been introduced to describe the characterization of phonon scattering at such boundaries, and it can be expressed as $P = \exp(-16\pi^3\Delta^2/\lambda^2)$ [8], in which Δ is the root-mean-square value of the roughness fluctuations and λ is dominant phonon wavelength. When P is equal to 1, the phonon scattering is completely specular, while $P = 0$ corresponds to the diffusive scattering. According to Ref. [30], the dominant phonon wave length decreases with increasing temperature. For silicon at room temperature, the dominant phonon wave length is approximately less than 1 nm [25], and thus any realistic surface roughness will make P equal to 0. Therefore, the phonon-boundary scattering at the pore boundaries is set as completely diffusive.

3. Theoretical model

In the classical Fourier's law based model for macroporous materials, the effective thermal conductivity, $k_{\text{eff,bulk}}$, for the given pore shape and heat flux direction is only a function of porosity, $k_{\text{eff,bulk}} = k_{\text{bulk}}F(\varepsilon)$, where k_{bulk} is the bulk thermal conductivity of host material and $F(\varepsilon)$ describes the porosity dependence of thermal conductivity. In the case shown in Fig. 1(a), according to the effective medium approach (EMA) [11,31], we have $F(\varepsilon) = 1 - \varepsilon$ and then

$$k_{\text{eff,bulk}} = [1 - \varepsilon]k_{\text{bulk}}, \tag{2}$$

which indicates that the effective thermal conductivity linearly decreases with the increasing porosity. However, owing to phonon boundary scattering at pore boundaries, the effective thermal conductivity of nanoporous materials does not obey this variation rule, and becomes dependent on the pore radius. Besides, for nanoporous thin films where the scale of temperature gradient can be comparable to the phonon MFP, ballistic transport also leads to the thickness-dependence of effective thermal conductivity [23]. Therefore, the effective thermal conductivity of nanoporous thin films should be expressed as

$$k_{\text{eff}} = [1 - \varepsilon]k_{\text{m}}(R_p, \varepsilon, L_x), \tag{3}$$

in which the effective thermal conductivity of host material, $k_{\text{m}}(R_p, \varepsilon, L_x)$, is related to the pore radius, the porosity and the film thickness simultaneously. Here, an analytical model for $k_{\text{m}}(R_p, \varepsilon, L_x)$ is derived on the basis of the phonon BTE. For a multiply-constrained nanostructure (e.g. nanoporous thin film), an analytical solution of the phonon BTE is rather difficult to obtain when simultaneously considering all the constraints. Therefore, in order to derive a relatively simple but efficient thermal conductivity model for nanoporous thin film, we deal with the size effects due to the film thickness and the pore radius separately, and then combine them by using Matthiessen's rule [32].

3.1. Size effect resulting from the pore-boundary scattering

First consider the size effect resulting from the pore boundary scattering. The corresponding phonon BTE is [8,32]

$$v_{gx}\frac{\partial f_0}{\partial T}\frac{dT}{dx} + \vec{v}_{gr}\cdot\nabla_r f_1 = \frac{-f_1}{\tau}, \tag{4}$$

in which $f_1 = f - f_0$, $\vec{r} = (y, z)$ is the planar position vector, ∇_r refers to $\partial/\partial y + \partial/\partial z$, and $\vec{v}_{gr} = (v_{gy}, v_{gz})$ is the planar group velocity vector. The temperature gradient along the x-direction (dT/dx) is not varied, and the term $\partial f_1/\partial x$ vanishes neglecting the influence of x-directional constraints. Besides, the diffusive scattering boundary condition at the pore boundaries is written as $f_1(\vec{r}_B)_{v_{gr,n}} = 0$ where the position vector, $\vec{r}_B = (y_B, z_B)$, describes the profile of pore boundaries. Then, Eq. (4) has a solution [8,33]:

$$f_1 = v_{gx}\tau \frac{\partial f_0}{\partial T}\frac{dT}{dx}\left(\exp\left(-\frac{L_{rp}}{v_{gr}\tau}\right) - 1\right), \tag{5}$$

where $v_{gr} = \sqrt{v_{gy}^2 + v_{gz}^2} = v_g \sin(\theta)$ with θ representing the polar angle between the phonon traveling direction and the x-axis, and L_{rp} is the length from the location r of the integration in the cross section to the point p at the pore boundaries [33].

The diffusive scattering at the pore boundaries directly suppresses the phonon transport, while the specular scattering at the outer boundaries only changes the direction of $\vec{v}_{gr}$ to increase the diffusive scattering rate at the pore boundaries. Therefore, as shown in Fig. 3, there are three kinds of L_{rp} for this periodic pore structure. Fig. 3(a) illustrate the first kind of L_{rp}, which corresponds to that the phonon directly arrives at the pore boundaries. Then, we have

$$L_{rp1} = r\left[|\cos\varphi| - \left(\left(\frac{R_p}{r}\right)^2 - \sin^2\varphi\right)^{1/2}\right], \quad \pi - \varphi_{c1} \leqslant \varphi \leqslant \pi + \varphi_{c1}, \tag{6}$$

in which φ is the azimuth angle, and the critical angle is $\varphi_{c1} = \arcsin(R_p/r)$. The second kind of L_{rp} as shown in Fig. 3(b) represents that the phonon arrives at the pore boundaries after the specular scattering at the outer boundaries, and is calculated as

$$L_{rp2} = \frac{R_p}{\sqrt{\varepsilon}}\frac{\sin(\varphi - \varphi_2)}{\sin(\varphi)} + \frac{R_p}{\sqrt{\varepsilon}}\left[|\cos\varphi_2| - (\varepsilon - \sin^2\varphi_2)^{1/2}\right], \quad 0 \leqslant \varphi \leqslant \varphi_{c1} \text{ or } 2\pi - \varphi_{c1} < \varphi \leqslant 2\pi \tag{7}$$

with $\varphi_2 = \arcsin[(r\sqrt{\varepsilon}/R_p)\sin(\varphi)]$. Besides, Fig. 3(c) shows the third kind of L_{rp}, corresponding to that the phonon cannot arrive at the pore boundaries even after the specular scattering at the outer boundaries. In this case, we have

$$L_{rp3} = \infty, \ \varphi_{c1} \leqslant \varphi \leqslant \pi - \varphi_{c1} \text{ or } \pi + \varphi_{c1} < \varphi \leqslant 2\pi - \varphi_{c1}. \tag{8}$$

The x-directional heat flow is calculated as

$$Q_x = \int dS_A \int_0^{2\pi}\int_\pi^0\int_0^{\omega_m} v_g \omega\hbar f_1 \cos(\theta) D(\omega) d\omega d\cos(\theta) d\varphi, \tag{9}$$

where S_A is the cross sectional area, ω is the angle frequency, $\hbar$ is the Dirac constant, and $D(\omega)$ is the density of states (DOS). For clarity, the Debye approximation is applied, and the combining of Eqs. (5) and (9) then leads to

$$Q_x = \frac{C_v l v_g}{4\pi}\frac{dT}{dx}\int_{S_A} dS_A \int_0^{2\pi}\int_{-1}^{1}\left(\exp\left(-\frac{L_{rp}}{l_0\sqrt{1-\mu^2}}\right) - 1\right)\mu^2 d\mu d\varphi \tag{10}$$

in which C_V is the heat capacity, $l_0 = v_g\tau$ is the intrinsic phonon MFP, and $\mu = \cos(\theta)$. Then, using Fourier's law, we can obtain the effective thermal conductivity of the host material considering the pore radius dependence,

$$k_{m,p} = \frac{Q_x}{S_A}\Big/\left(-\frac{dT}{dx}\right) = \frac{k_{bulk}}{G}, \tag{11}$$

with $k_{bulk} = C_v l_0 v_g/3$ and

$$G^{-1} = 1 - \frac{3}{\pi R_p^2(\varepsilon^{-1} - 1)}\int_{R_p}^{R_p/\sqrt{\varepsilon}} r dr \int_0^{2\pi}\int_0^1 \exp\left(-\frac{L_{rp}}{l_0\sqrt{1-\mu^2}}\right)\mu^2 d\mu d\varphi. \tag{12}$$

Here, we should note that what really matters for the pore boundary scattering is the ratio between the pore separation distance ($2[R_o - R_p]$) and the phonon MFP. The function G can be easily rearranged as a function of the separation distance and the porosity, using the equation, $1/2(\varepsilon^{-1/2} - 1)R_p = R_o - R_p$. Nevertheless, when the porosity is given, the separation distance is directly dependent on the pore radius, and this is the reason why some researchers [10] chose to study the effective thermal conductivity varying with pore radius.

3.2. Size effect resulting from film thickness

When considering the film thickness dependence of effective thermal conductivity, the corresponding phonon BTE [29,32] is

$$v_g\mu\frac{\partial f}{\partial x} = \frac{f_0 - f}{\tau} \tag{13}$$

with the boundary conditions, $f(0) = f_0(T_1)$ and $f(L_x) = f_0(T_2)$, in which T_1 and T_2 are the temperatures of phonon baths, respectively. Eq. (13) is the one-dimensional form of the phonon BTE, Eq. (1). In Eq. (13), the influence of pore boundary-scattering in the yz plane is not included, and only the ballistic transport is taken into account [29,32]. Besides, Eq. (13) can be solved through the differential approximation with the temperature jump boundary conditions [34,35]. Then, the effective thermal conductivity, considering the film thickness dependence, is given by

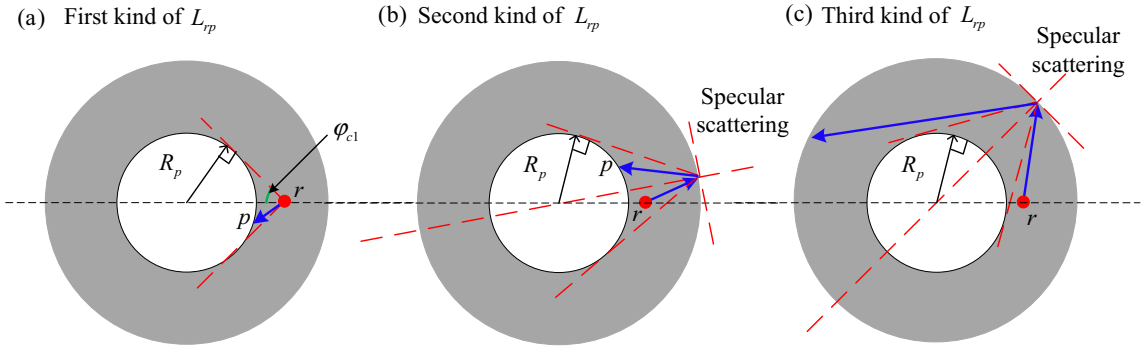

Fig. 3. Schematics for three kinds of L_{rp}: L_{rp} is the length from the location r to the point p at the pore boundaries, and $\varphi_{c1} = \arcsin(R_p/r)$.

$$k_{m,t} = \frac{k_{bulk}}{1 + \frac{4}{3}\frac{l_0}{L_x}}. \quad (14)$$

In early 1993, Majumdar [29] introduced Eq. (14) to characterize the cross-plane thermal conductivity of nanofilms, and then this expression has been extensively applied [36].

3.3. Combination of both effects through Matthiessen's rule

The size effects due to the film thickness and the pore radius can be combined by using Matthiessen's rule. According to Matthiessen's rule, when the coupling effects between different scattering mechanisms can be neglected, the total confined MFP caused by the longitudinal (x-direction) constraints and the pore boundary scattering is

$$l_m^{-1} = l_0^{-1} + l_x^{-1} + l_p^{-1}, \quad (15)$$

where l_x is the longitudinal constrained MFP, and l_p is the confined MFP resulting from the pore boundary scattering. In principle, the ratio of the size-dependent effective thermal conductivity to the bulk value is calculated as

$$\frac{k_m}{k_{bulk}} = \frac{l_m}{l_0} = \frac{1}{1 + \frac{l_0}{l_x} + \frac{l_0}{l_p}}. \quad (16)$$

We deal with the size effects due to the pore radius and the film thickness separately, and obtain the corresponding effective thermal conductivity expressions, i.e. Eqs. (11) and (14). According to Matthiessen's rule, when only one boundary scattering mechanism exist in the system, the effective thermal conductivity should be expressed in the form as, $k_{m,p(t)}/k_{bulk} = [1 + l_0/l_{x(p)}]^{-1}$, where $l_{p(x)}$ (l_p or l_x) is the corresponding confined MFP. Therefore, by converting Eqs. (11) and (14) into the form of Matthiessen's rule, we can obtain the corresponding confined MFPs, i.e. l_p and l_x, respectively. We convert Eq. (11) into the form of Matthiessen's rule as $k_{m,p}/k_{bulk} = 1/(1 + l_0/l_p) = G^{-1}$, and thus obtain $l_p = l_0/(G - 1)$. Following the similar procedures above, the longitudinal constrained MFP is calculated as $l_x = 3L_x/4$, referring to Eq. (14). Finally, combining Eqs. (3) and (16), we can have the analytical model for the effective thermal conductivity of nanoporous thin films,

$$\frac{k_{eff}}{k_{bulk}} = \frac{1 - \varepsilon}{G + \frac{4}{3}\frac{l_0}{L_x}}, \quad (17)$$

with the characteristic lengths (both L_x and R_p) increasing, we have $l_0/L_x \to 0$ as well as $G \to 1$, and Eq. (17) gradually reduces to the EMA model, Eq. (3), for macroporous materials.

It is straightforward to extend Eq. (17) to take the phonon dispersion into account. At room temperature, the contribution of momentum-conserving collisions (normal scattering) can be assumed to be negligible for three-dimensional materials [37], so the standard relaxation time approximation model [38] can be used,

$$k_{eff} = \frac{1 - \varepsilon}{3}\sum_j \int_0^{\omega_{mj}} \hbar\omega \frac{\partial f_0}{\partial T} v_{gj} l_{mj} D_j(\omega) d\omega, \quad (18)$$

with $l_{mj} = l_{0j} \Big/ \left(G(l_{0j}, R_p, \varepsilon) + \frac{4}{3}\frac{l_{0j}}{L_x}\right)$, where l_{0j} is the intrinsic phonon MFP of frequency ω and polarization j, and the modified MFP l_{mj} reflects the size effects due to the film thickness and the pore radius. Besides, another efficient way to consider the phonon dispersion is to use the phonon MFP spectra function [39],

$$k_{eff} = [1 - \varepsilon] \int_0^{\infty} \phi_{l_{0\omega}} H(l_{0\omega}, R_p, \varepsilon, L_x) dl_{0\omega} \quad (19)$$

where $\phi_{l_{0\omega}}$ is differential MFP spectra function which has been measured in experiments [40], and $H(l_{0\omega}, R_p, \varepsilon, L_x)$ is the suppression function exactly equal to

$$H(l_{0\omega}, R_p, \varepsilon, L_x) = \frac{l_{m\omega}}{l_{0\omega}} = \frac{1}{G(l_{0\omega}, R_p, \varepsilon) + \frac{4}{3}\frac{l_{0\omega}}{L_x}}. \quad (20)$$

It is noted that our model considers the ballistic transport and the pore boundary scattering but not the coherent phononic effects [20,21,28] at present. In fact, the modifications of phonon properties due to the phononic crystal patterning (e.g. shift of DOS and reduction of group velocity) can be further taken into account via using the corresponding phonon MFP spectra function.

4. Comparison with MC simulations

A MC technique [41,42] is employed to simulate the phonon transport in the nanoporous silicon thin films. It is noted that the MC technique simulates phonon transport through random number samplings, equivalent to directly solving the phonon BTE. In our simulations, the intensity of each phonon bundle emitting from the boundary is defined as, $W = E/N$, where E is the total emitting phonon energy dependent on the temperature of phonon bath, and N is the number of phonon bundles that we trace in the simulations. N must be enough large to preserve the simulation accuracy. And it is set 10^8 in the present work. The traveling direction vector of the phonon bundle is expressed as $\vec{s} = \cos(\theta)\vec{i} + \sin(\theta)\cos(\varphi)\vec{j} + \sin(\theta)\sin(\varphi)\vec{k}$. As the phonon bundle emits form the boundary, $\sin\theta = \sqrt{\gamma_\theta}$, $\varphi = 2\pi\gamma_\varphi$, γ_θ and γ_φ are independent random numbers which range from 0 to 1. While as the phonon bundle travels in the media, $\cos\theta = 1 - 2\gamma_\theta$, $\varphi = 2\pi\gamma_\varphi$ [34]. The phonon tracing algorithm is as follows: (1) Draw the initial properties (e.g. position r_0 of phonons). (2) Calculate the traveling length, Δr, until the first scattering event ($\Delta r = -l_0 \ln(\gamma)$, where γ is the uniformly random number ranging from 0 to 1), and renew the position of phonons, $r_{new} = r_0 + \Delta r$. (3) If a phonon collides with a boundary at r_B, set $r_{new} = r_B$; In terms of the nature of the boundary, we can determine whether the phonon reemits from the boundary. (4) If a phonon does not collide with boundaries, the phonon should reemit at r_{new}, and set $r_0 = r_{new}$. (5) If the phonon arrives at the absorbing boundaries (e.g. black-body boundaries), the tracing process of this phonon is finished, then we proceed to (1) and begin the tracing of the next phonon. Besides, the heat flow is calculated by counting the number of phonons arriving at the isothermal boundary at $x = L_x$.

The Debye approximation is adopted to deal with the phonon properties of silicon at the room temperature, and thus phonons travel with one average group velocity and the scattering rate is characterized by an average phonon MFP. We choose the average MFP as 260 nm with its corresponding heat capacity (0.93×10^6 J/m^3 K) and average group velocity (1800 m/s) [43]. This average MFP is obtained by considering the dispersion of the acoustic phonons and neglecting the optical phonon contribution to the thermal conductivity [43]. And it is consistent with experiments of Ju and Goodson [44]. In fact, although arguments still exist on the value of the average phonon MFP of silicon at room temperature, the choice of MFP does not influence the comparisons between the MC simulations and the present model owing to that all quantities in both the MC simulations and the theoretical model are dimensionless.

Our model, Eq. (17), can be verified by comparison with the MC simulation results. All quantities in Figs. 4–7 are converted into dimensionless, and the Knudsen numbers are defined as $Kn_L = l_0/L_x$ and $Kn_R = l_0/R_p$. Figs. 4 and 5 show the cross-plane effective thermal conductivity of nanoporous silicon thin films

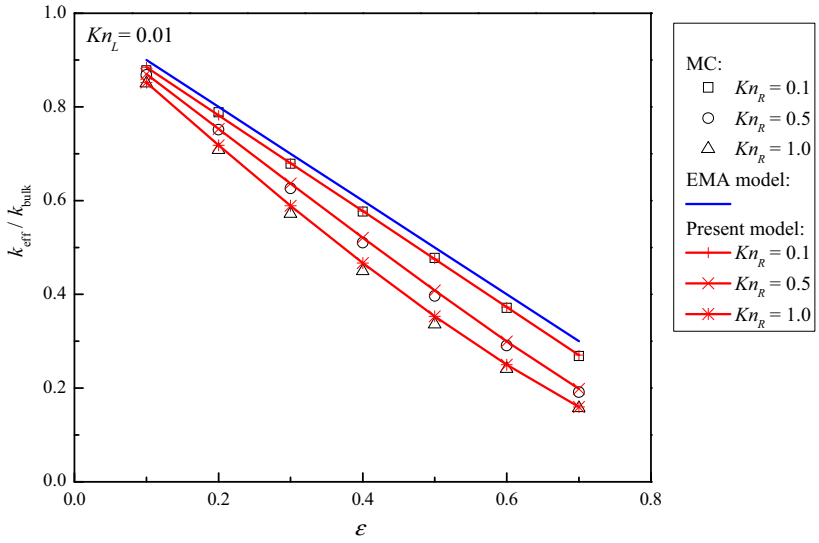

Fig. 4. Cross-plane effective thermal conductivity of nanoporous silicon thin films with different pore radii ($Kn_R = 0.1, 0.5, 1.0$) and a given thickness ($Kn_L = 0.01$) along the pore axial direction as a function of porosity (ε).

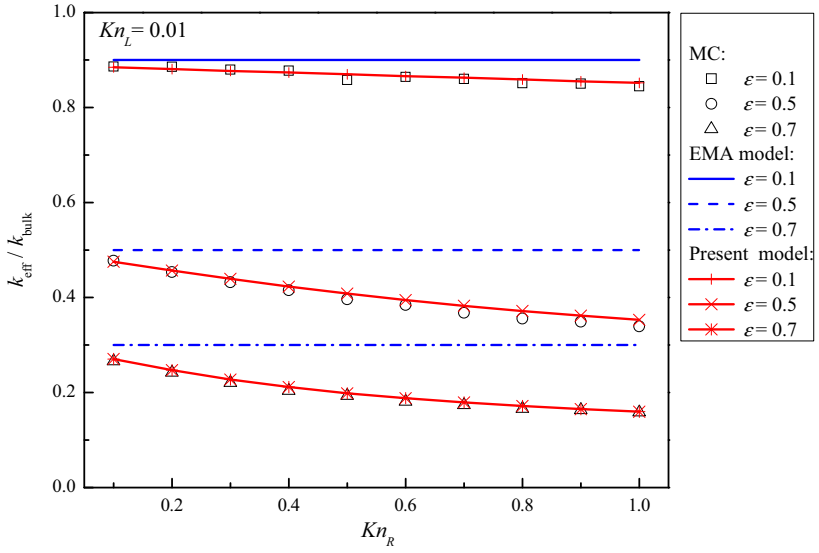

Fig. 5. Cross-plane effective thermal conductivity of nanoporous silicon thin films with different porosities ($\varepsilon = 0.1, 0.5, 0.7$) and a given thickness ($Kn_L = 0.01$) along the pore axial direction as a function of pore radius (Kn_R).

with a given thickness as a function of porosity and pore radius. Since the film thickness is rather larger than the phonon MFP, i.e. $Kn_L = 0.01$, the size effect due to the thickness can be neglected. As shown in Fig. 4, the EMA model, Eq. (2), is invalid for nanoporous films, that is, the effective thermal conductivity does not linearly decrease with the increasing porosity ε, and becomes dependent on the Knudsen number Kn_R. With the Knudsen number Kn_R decreasing, the present model can be gradually reduced to the EMA model. Phonon-boundary scattering at the pore boundaries causes the size-dependence of host material thermal conductivity (k_m), resulting in the further reduction of effective thermal conductivity, which has been proved by Hopkins et al. [21] in experiments. Besides, the larger the Knudsen number Kn_R (that is, the smaller the pore radius R_p), the more remarkable is the deviation of variation rule from that predicted by the EMA model. The good agreements between the MC simulations and the present model indicate that the function, G, can well reflect the effect of pore boundary scattering on the phonon transport. Fig. 5 suggests that the effective thermal conductivity of nanoporous films decreases with the increasing Knudsen number Kn_R for the given porosity. It is found that decreasing the porosity can enhance the pore radius dependence of effective thermal conductivity. Besides, the present model can also accurately predict the MC simulation results. With the decreasing Kn_R, the effect of boundary scattering at pore boundaries gradually vanishes, and the present model is degrading to the EMA model, Eq. (3), for macroporous materials.

Fig. 6 shows the effective thermal conductivity of nanoporous silicon thin films with the given porosity ($\varepsilon = 0.5$) as a function of film thickness (Kn_L). With the Knudsen number Kn_L increasing (that is, the thickness decreasing), the scale of temperature gradient becomes comparable to the phonon MFP, and the influence of ballistic transport can also reduce the effective thermal conductivity. The effective thermal conductivity decreases with the increasing Kn_L, despite of the different Kn_R. Our model slightly

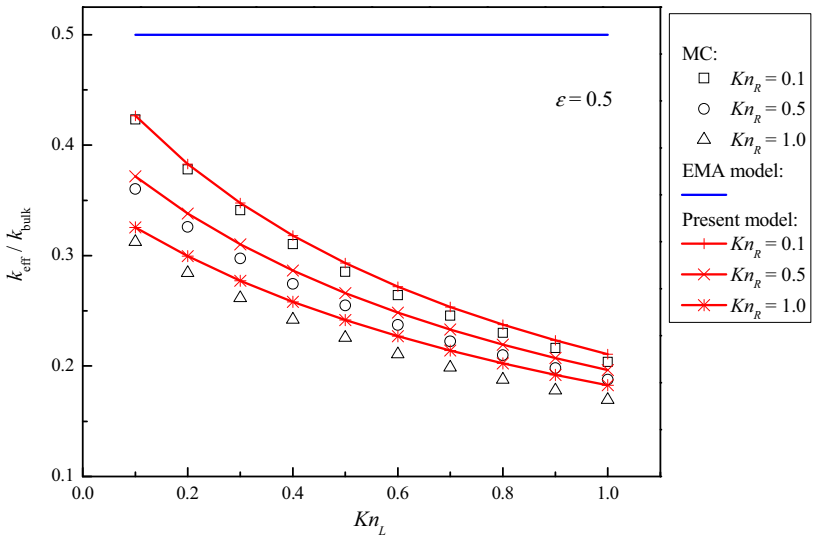

Fig. 6. Cross-plane effective thermal conductivity of nanoporous silicon thin films with different pore radii ($Kn_R = 0.1, 0.5, 1.0$) and a given porosity ($\varepsilon = 0.5$) along the pore axial direction as a function of thickness (Kn_L).

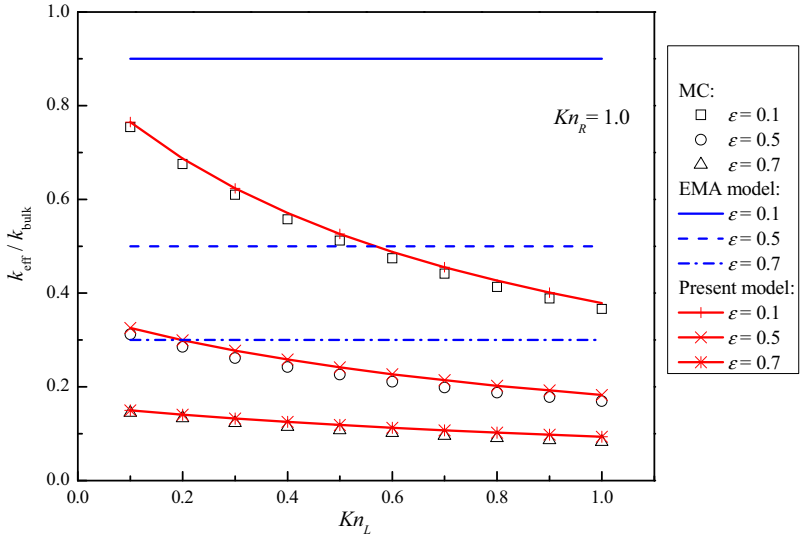

Fig. 7. Cross-plane effective thermal conductivity of nanoporous silicon thin films with different porosities ($\varepsilon = 0.1, 0.5, 0.7$) and a given pore radius ($Kn_R = 1.0$) along the pore axial direction as a function of thickness (Kn_L).

over-predicts the results obtained by the MC simulations in the region of large Knudsen number Kn_L, and the deviation (only about 5%) may mainly result from the differential approximation which is employed to obtain Eq. (14) [32,45]. The deviation can be improved by using the modified differential approximation method [32,45], but the modification can lead to a rather complicated expression. Actually, this small deviation will not influence the practical applications of our model.

Fig. 7 shows the effective thermal conductivity of nanoporous silicon thin films with the given pore radius ($Kn_R = 1.0$) as a function of film thickness Kn_L. It is also found that the effective thermal conductivity decreases with the increasing Kn_L, despite of the different porosity, and the effective thermal conductivity can be significantly reduced when compared to the results predicted by the EMA model. In the region of larger Knudsen number Kn_L where the phonon ballistic transport dominates, the effective thermal conductivity is mainly dependent on the film thickness, which has been demonstrated in the experiments of Lee et al. [23]. The good agreements between the MC simulations and the present model further verify the validity of the model. Furthermore, it should be noted that we combine the size effects due to the different constraints by using Matthiessen's rule which assumes that the different scattering progresses are independent. Although this assumption cannot always be valid [46], the present model's good agreements with the MC simulations have demonstrated that the coupling effect is not significant in our studying cases.

5. Conclusions

Nanoporous silicon thin films have demonstrated great potential in highly-efficient thermoelectric materials, necessitating the in-depth study on their thermal properties. In the present work, we have derived an analytical model for the cross-plane effective thermal conductivity of nanoporous thin films based on the phonon BTE. The size effects caused by different constraints are dealt

with separately, and then combined via using Matthiessen's rule. The present model can capture the size effects due to the film thickness and the pore radius simultaneously. The effective thermal conductivity of nanoporous silicon does not obey the variation rule predicted by the EMA model for macroporous materials. And it is significantly reduced due to the pore boundary scattering and phonon ballistic transport. The smaller the film thickness or the pore radius, the smaller is the effective thermal conductivity for a given porosity. Moreover, the good agreements between the present model and the MC simulations have been achieved, indicating the validity of our model. Results of our work can provide a more in-depth understanding about the heat conduction in nanoporous silicon films, and the present model can be directly used to develop highly-efficient thermoelectric devices.

Acknowledgements

This work is financially supported by National Natural Science Foundation of China (Nos. 51322603, 51136001, 51356001), and Science Fund for Creative Research Group (No. 51321002), the Tsinghua National Laboratory for Information Science and Technology of China (TNList).

References

[1] M.H. Elsheikh, D.A. Shnawah, M.F.M. Sabri, et al., A review on thermoelectric renewable energy: principle parameters that affect their performance, Renew. Sustain. Energy Rev. 30 (2014) 337–355.
[2] H.B. Gao, G.H. Huang, H.J. Li, et al., Development of stove-powered thermoelectric generators: a review, Appl. Therm. Eng. 96 (2016) 297–310.
[3] C. Goupil, W. Seifert, K. Zabrocki, et al., Thermodynamics of thermoelectric phenomena and applications, Entropy 13 (2011) 1481–1517.
[4] E.S. Toberer, A. Zevalkink, G.J. Snyder, Phonon engineering through crystal chemistry, J. Mater. Chem. 21 (2011) 15843.
[5] H. Alam, S. Ramakrishna, A review on the enhancement of figure of merit from bulk to nano-thermoelectric materials, Nano Energy 2 (2013) 190–212.
[6] C. Sanchez, C. Boissière, D. Grosso, C. Laberty, et al., Design, synthesis, and properties of inorganic and hybrid thin films having periodically organized nanoporosity, Chem. Mater. 20 (2010) 682–737.
[7] G. Galli, D. Donadio, Thermoelectric materials: silicon stops heat in its tracks, Nat. Nanotechnol. 5 (2010) 701–702.
[8] J. Ziman, Electrons and Phonons, Oxford University Press, London, 1961.
[9] D.G. Cahill, P.V. Braun, G. Chen, et al., Nanoscale thermal transport. II. 2003–2012, Appl. Phys. Lett. 1 (2014) 011305.
[10] E. Pop, Energy dissipation and transport in nanoscale devices, Nano Res. 3 (2010) 147–169.
[11] R. Yang, G. Chen, M.S. Dresselhaus, Thermal conductivity of simple and tubular nanowire composites in the longitudinal direction, Phys. Rev. B 72 (2005) 125418.
[12] T.Y. Hsieh, H. Lin, T.J. Hsieh, et al., Thermal conductivity modeling of periodic porous silicon with aligned cylindrical pores, J. Appl. Phys. 111 (2012) 124329.
[13] G.H. Tang, C. Bi, B. Fu, Thermal conduction in nano-porous silicon thin film, J. Appl. Phys. 114 (2013) 184302.
[14] J.H. Lee, G.A. Galli, J.C. Grossman, Nanoporous Si as an efficient thermoelectric material, Nano Lett. 15 (2008) 3750–3754.
[15] J. Fang, L. Pilon, Tuning thermal conductivity of nanoporous crystalline silicon by surface passivation: a molecular dynamics study, Appl. Phys. Lett. 101 (2012) 011909.
[16] J. Randrianalisoa, D. Baillis, Monte Carlo simulation of cross-plane thermal conductivity of nanostructured porous silicon films, J. Appl. Phys. 103 (2008) 053502.
[17] L.C. Liu, M.J. Huang, Thermal conductivity modeling of micro- and nanoporous silicon, Int. J. Therm. Sci. 49 (2010) 1547–1554.
[18] S. Wolf, N. Neophytou, H. Kosina, Thermal conductivity of silicon nanomeshes: effects of porosity and roughness, J. Appl. Phys. 115 (2014) 204306.
[19] J.K. Yu, S. Mitrovic, D. Tham, et al., Reduction of thermal conductivity in phononic nanomesh structures, Nat. Nanotechnol. 5 (2010) 718–721.
[20] S. Alaie, D.F. Goettler, M. Su, et al., Thermal transport in phononic crystals and the observation of coherent phonon scattering at room temperature, Nat. Commun. 6 (2015) 7228.
[21] P.E. Hopkins, C.M. Reinke, M.F. Su, et al., Reduction in the thermal conductivity of single crystalline silicon by phononic crystal patterning, Nano Lett. 11 (2011) 107–112.
[22] J.M. Weisse, A.M. Marconnet, D.R. Kim, et al., Thermal conductivity in porous silicon nanowire arrays, Nanoscale Res. Lett. 7 (2012) 554.
[23] J. Lee, J. Lim, P. Yang, Ballistic phonon transport in holey silicon, Nano Lett. 15 (2015) 3273–3279.
[24] R. Prasher, Transverse thermal conductivity of porous materials made from aligned nano- and microcylindrical pores, J. Appl. Phys. 100 (2006) 064302.
[25] R. Prasher, Thermal conductivity of composites of aligned nanoscale and microscale wires and pores, J. Appl. Phys. 100 (2006) 034307.
[26] F.X. Alvarez, D. Jou, A. Sellitto, Pore-size dependence of the thermal conductivity of porous silicon: a phonon hydrodynamic approach, Appl. Phys. Lett. 97 (2010) 033103.
[27] R. Dettori, C. Melis, X. Cartoixà, et al., Model for thermal conductivity in nanoporous silicon from atomistic simulations, Phys. Rev. B 91 (2015) 054305.
[28] E. Dechaumphai, R. Chen, Thermal transport in phononic crystals: the role of zone folding effect, J. Appl. Phys. 111 (2012) 073508.
[29] A. Majumdar, Microscale heat conduction in dielectric thin films, J. Heat Transf. 115 (1993) 7–16.
[30] V. Yefremenko, G. Wang, V. Novosad, et al., Low temperature thermal transport in partially perforated silicon nitride membranes, Appl. Phys. Lett. 94 (2009) 183504.
[31] C.W. Nan, R. Birringer, D.R. Clarke, et al., Effective thermal conductivity of particulate composites with interfacial thermal resistance, J. Appl. Phys. 81 (1997) 6692.
[32] Y.C. Hua, B.Y. Cao, Ballistic-diffusive heat conduction in multiply-constrained nanostructures, Int. J. Therm. Sci. 101 (2016) 126–132.
[33] D. Josell, C. Burkhard, Y. Li, et al., Electrical properties of superfilled submicrometer silver metallizations, J. Appl. Phys. 96 (2004) 759–768.
[34] Y.C. Hua, B.Y. Cao, Phonon ballistic-diffusive heat conduction in silicon nanofilms by Monte Carlo simulations, Int. J. Heat Mass Transf. 78 (2014) 755–759.
[35] J. Maassen, M. Lundstrom, Steady-state heat transport: ballistic-to-diffusive with Fourier's law, J. Appl. Phys. 117 (2015) 035104.
[36] A.J.H. McGaughey, E.S. Landry, D.P. Sellan, et al., Size-dependent model for thin film and nanowire thermal conductivity, Appl. Phys. Lett. 99 (2011) 131904.
[37] S. Lee, D. Broido, K. Esfarjani, et al., Hydrodynamic phonon transport in suspended graphene, Nat. Commun. 6 (2015) 6290.
[38] N. Mingo, Calculation of Si nanowire thermal conductivity using complete phonon dispersion relations, Phys. Rev. B 68 (2003) 113308.
[39] F. Yang, C. Dames, Mean free path spectra as a tool to understand thermal conductivity in bulk and nanostructures, Phys. Rev. B 87 (2013) 035437.
[40] Y. Hu, L. Zeng, A.J. Minnich, et al., Spectral mapping of thermal conductivity through nanoscale ballistic transport, Nat. Nanotechnol. 10 (2015) 701–706.
[41] J.P.M. Péraud, N.G. Hadjiconstantinou, An alternative approach to efficient simulation of micro/nanoscale phonon transport, Appl. Phys. Lett. 101 (2012) 153114.
[42] Y.C. Hua, Y. Dong, B.Y. Cao, Monte Carlo simulation of phonon ballistic diffusive heat conduction in silicon nanofilm, Acta Phys. Sin. 62 (2013) 244401.
[43] G. Chen, Thermal conductivity and ballistic-phonon transport in the cross-plane direction of superlattices, Phys. Rev. B 57 (1998) 14958.
[44] Y.S. Ju, K.E. Goodson, Phonon scattering in silicon films with thickness of order 100 nm, Appl. Phys. Lett. 74 (1999) 3005.
[45] D. Olfe, A modification of the differential approximation for radiative transfer, AIAA J. 5 (1967) 638–643.
[46] J. Glasbrenner, B. Pujari, K. Belashchenko, Deviations from Matthiessen's rule and resistivity saturation effects in Gd and Fe from first principles, Phys. Rev. B 89 (2014) 174408.